Supplementary information

Effective electro-optical modulation with high extinction ratio by a graphene-silicon microring resonator

Yunhong Ding,[*1] Xiaolong Zhu,[1,2] Sanshui Xiao,[1,2] Hao Hu,[1] Lars Hagedorn Frandsen,[1] N. Asger Mortensen,[1,2] Kresten Yvind[1]

[1]Department of Photonics Engineering, Technical University of Denmark, DK-2800 Kongens Lyngby, Denmark

[2]Center for Nanostructured Graphene, Technical University of Denmark, DK-2800 Kongens Lyngby, Denmark

yudin@fotonik.dtu.dk

Contents

1. **Theory and calculation of propagation loss…………………………………………….. 2**
2. **Theory for microring resonator calculation………………………………………….. 3**
3. **Fabrication process………………………………………………………….……….. 4**
4. **Raman spectroscopy…………………………………………………………………. 7**
5. **Experimental setup…………………………………………………..……………… 7**
6. **Comparison between TE and TM mode……………………………..………………8**
7. **References…………………………………………………………….……………… 9**

1. Theory and calculation of propagation loss

The dimension of the designed waveguide with air cladding is shown in Fig. S1.

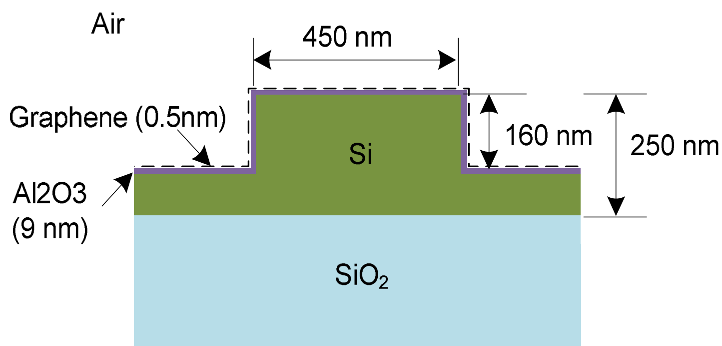

Fig. S1. Cross section of the designed graphene-silicon waveguide.

The width of the waveguide is designed to be 450 nm, and the etching depth is 160 nm. The Al2O3 is designed to be 9 nm thick, and the thickness of the graphene sheet is considered to be 0.5 nm [S1]. With the aid of the random phase approximation and the Kramers-Kronig relations, the Fermi level E_f dependent complex dielectric constant ($\varepsilon_G = \varepsilon'_G + j\varepsilon''_G$) of graphene can be described by as [S2]

$$\begin{aligned}
\varepsilon'_G\left(E_p\right) &= 1 + \frac{e^2}{8\pi E_p \varepsilon_0 d} \ln \frac{\left(E_p + 2\left|E_f\right|\right)^2 + \Gamma^2}{\left(E_p - 2\left|E_f\right|\right)^2 + \Gamma^2} - \frac{e^2}{\pi \varepsilon_0 d} \frac{\left|E_f\right|}{E_p^2 + \left(1/\tau\right)^2} \\
\varepsilon''_G\left(E_p\right) &= \frac{e^2}{4 E_p \varepsilon_0 d}\left[1 + \frac{1}{\pi}\left(\tan^{-1}\frac{E_p - 2\left|E_f\right|}{\Gamma} - \tan^{-1}\frac{E_p + 2\left|E_f\right|}{\Gamma}\right)\right] + \frac{e^2}{\pi \tau E_p \varepsilon_0 d} \frac{\left|E_f\right|}{E_p^2 + \left(1/\tau\right)^2}
\end{aligned} \quad \text{(Eq.S1)}$$

where E_p is the photon energy, d is the thickness of graphene, Γ is the inter-band broadening, and $1/\tau$ is the free carrier scattering rate. Here the inter-band broadening is choosen as 160 meV, and the free carrier scattering rate $1/\tau$ becomes negligible when compared with the photon energy. The refractive indices of Si, SiO2 and Al2O3 are considered to be 3.45, 1.45, and 1.746, respectively. With the complex dielectric constant of graphene, the complex effective refractive index

($n_{eff} = n_{eff,real} + jn_{eff,imag}$), which consist of a real part $n_{eff,real}$ and imaginary part $n_{eff,imag}$, is calculated. The propagation is then obtained through

$$\alpha\left(dB/\mu m\right) = 2k_0 n_{eff,imag} \times 4.343\times10^{-6} \quad \text{(Eq.S2)}$$

where 4.343×10^{-6} is the constant for converting from m^{-1} to dB/μm.

2. Theory for microring resonator calculation

Considering an all-pass type microring resonator with graphene coverage-length of L, as shown in Fig. S2, the roundtrip transmission coefficient a, can be express as

$$a = \exp\left[-0.5\alpha_{Si}\left(2\pi R - L\right)\right]\exp\left(-0.5\alpha_{graphene-Si}L\right) \quad \text{(Eq.S3)}$$

where R is the radius of the microring resonator. α_{Si} and $\alpha_{graphene-Si}$ are the linear propagation loss of the pure silicon and graphene-silicon waveguide, respectively. The transmission can then be derived as [S3]

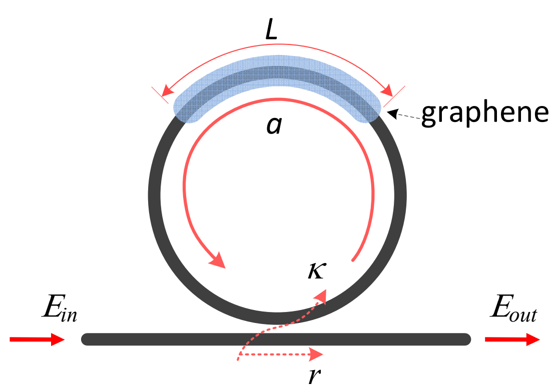

Fig. S2. All-pass type microring resonator with field coupling coefficient κ and roundtrip transmission coefficient *a*.

$$T_t = \left| \frac{E_{out}}{E_{in}} \right|^2_{\varphi=0} = \frac{r^2 + a^2 - 2ar\cos\varphi}{1 + a^2 r^2 - 2ar\cos\varphi} \quad \text{(Eq.S4)}$$

where φ is the roundtrip phase shift. r is the transmission coefficient of the coupling region of the microring, and $r = \sqrt{1-\kappa^2}$ for lossless coupling, where κ is the field coupling coefficient. The extinction ratio can be described as

$$ER_1 = 10\log_{10} \frac{(r+a)^2 (1-ar)^2}{(1+ar)^2 (r-a)^2} \quad \text{(Eq.S5)}$$

Considering a graphene coverage length of L and propagation loss tunability Δα, the roundtrip transmission coefficient after tuning graphene is

$$a'(\Delta\alpha) = a\exp(0.5\Delta\alpha L) \quad \text{(Eq.S6)}$$

Thus the responding transmission after tuning of graphene-silicon waveguide is

$$T_t(\Delta\alpha) = \frac{r^2 + a^2\exp(\Delta\alpha L) - 2ar\exp(0.5\Delta\alpha L)\cos\varphi}{1 + a^2 r^2 \exp(\Delta\alpha L) - 2ar\exp(0.5\Delta\alpha L)\cos\varphi} \quad \text{(Eq.S7)}$$

And the corresponding extinction ratio will be

$$ER_2 = 10\log_{10} \frac{\left[r - a\exp(0.5\Delta\alpha L)\right]^2 \left[1 + ar\exp(0.5\Delta\alpha L)\right]^2}{\left[1 - ar\exp(0.5\Delta\alpha L)\right]^2 \left[r + a\exp(0.5\Delta\alpha L)\right]^2} \quad \text{(Eq.S8)}$$

3. Fabrication process

The details of the fabrication process are shown in Fig. S3. A first SOI processing SOI processing, including e-beam lithography (EBL, JEOL JBX-9300FS, e-beam resist: ZEP520A) and inductively coupled plasma (ICP) etching (STS Advanced Silicon Etcher), was first used to fabricate the shallowly etched silicon microring resonators (Fig. S3(a)~S3(c)). Then second SOI processing is utilized to fabricate the fully etched regions where graphene and its contacts are placed (Fig. S3(d)~S3(e)). Standard UV lithography (photoresist: AZ5214E) is used afterwards to open the windows for the contacts on silicon (Fig. S(f)), and Au contact on silicon is formed by metal deposition and liftoff process (Fig. S3(g)~S3(h)). At the same time, PMMA is spin-coated onto the graphene covered copper foil and dried at 170 °C for 1 min (Fig. S3(i)~Fig. S3(j)). Following that, PMMA/graphene membrane is obtained by etching away the copper foil in a Fe(NO3)3/H2O solution, and transferred onto the silicon waveguide (Fig. S3(k)~S3(l)). Finally, the PMMA is dissolved in acetone and graphene wet transfer is finished (Fig. S3(m)~S3(n)). The graphene coverage area is then defined by standard UV lithography and followed by oxygen plasma etching and resist removing (Fig. S3(o)~S3(p)). The window for graphene contact is then defined by standard UV lithography Fig. S3(q), and Au/Cr contact on graphene is finally obtained by metal deposition and liftoff process (Fig. S3(r)~S3(s)).

During wet transfer, crack areas of graphene occur resulting in an imperfect coverage, as shown in Fig. S4. Such imperfect coverage leads to a lower propagation loss tunability of graphene-silicon waveguide, as explained in the manuscript.

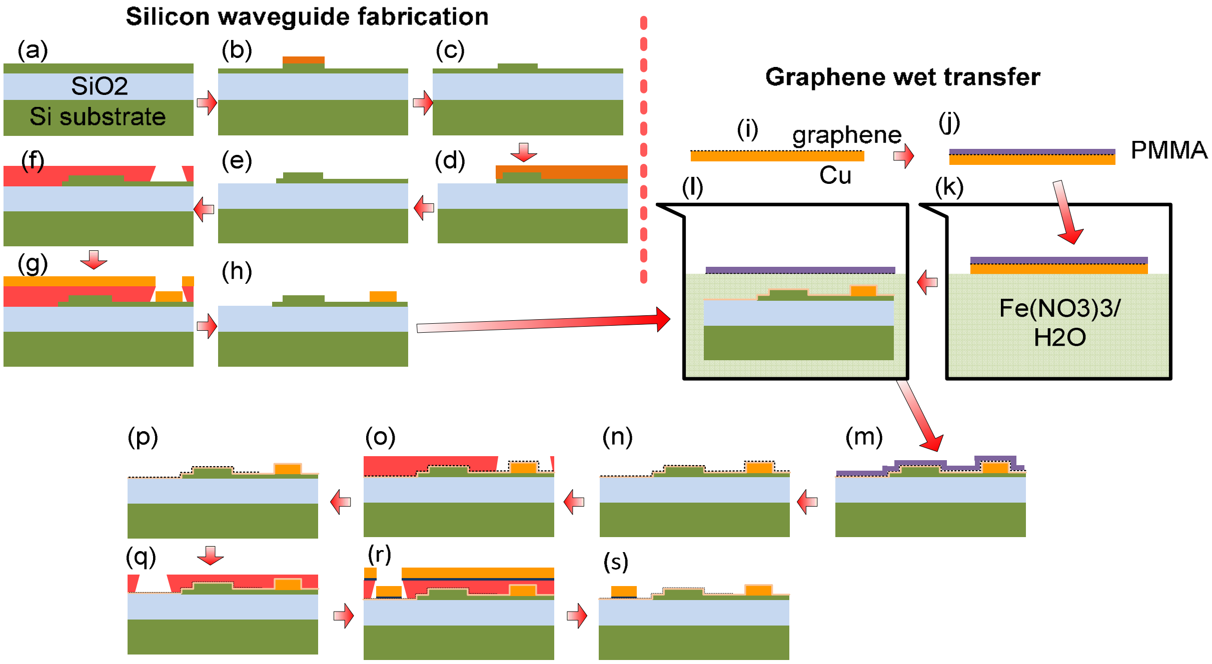

Fig.S3. Detailed fabrication process flow of the graphene-silicon device.

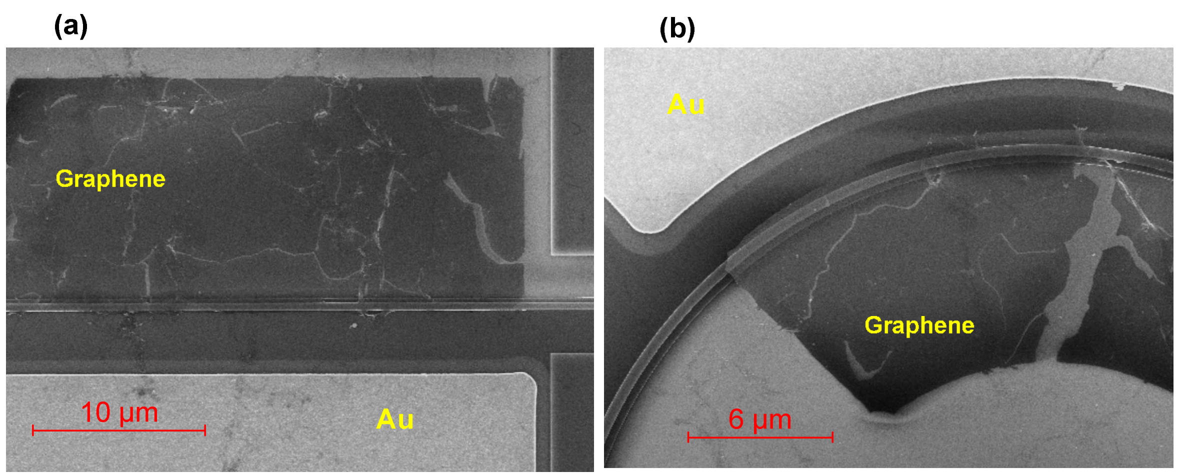

Fig. S4. SEM images of graphene-silicon straight waveguide (a) and ring waveguide (b) taken after defining graphene coverage (indicated in Fig. S3(p)), showing potential crack areas during wet transfer process.

4. Raman spectroscopy

The Raman spectroscopy is performed using a Thermo Scientific DXR Raman microscope with a 50× objective focusing a 532 nm lasers on the samples. The 532 nm laser power is kept at 1 mW for all measurements with an integration time of 1 s.

5. Experimental setup

The experimental setup for measuring the graphene-silicon devices is exhibited in Fig. S5. Light from a tunable laser source (TLS, ANDO AQ4321A) is polarization-tuned by a polarization controller (PC), and injected into the grating coupler on the TE mode for the waveguide. The light output from the chip is coupled to the output fiber by a grating coupler, and detected by the optical spectral analyzer (OSA, AQ6317B). The electrical contact for the silicon and graphene is connected to a power supply (Keithley 238, High Current Source Measure Unit). In the electro-optical switching experiment, the square waveform is generated by a waveform generator (Stanford Researcher Systems Inc., Model DG 535, Four Channel Digital Delay/Pulse Generator).

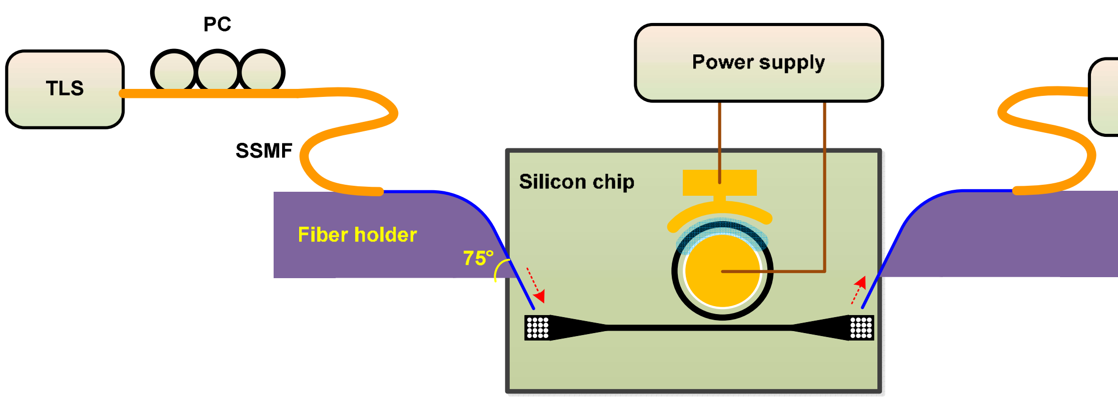

Fig. S5. Experimental setup for characterizing graphene-silicon devices.

6. Comparison between TE and TM mode

The propagation loss tunability of the TE and TM mode is compared. For the TE mode waveguide, the waveguide width is 450 nm as used in the manuscript. For the TM mode waveguide, the waveguide width is 700 nm, which is slightly narrower than that used in Y.T. Hu's demonstration. The etching depth is 160 nm for both TE and TM waveguide. The loss tunability of the TM mode waveguide shows slightly larger loss tunability of 0.06 dB/μm than the TE mode waveguide with loss tunability of 0.04 dB/μm. However, the TM mode waveguide also shows higher propagation loss, which agrees with Y.T.Hu's demonstration.

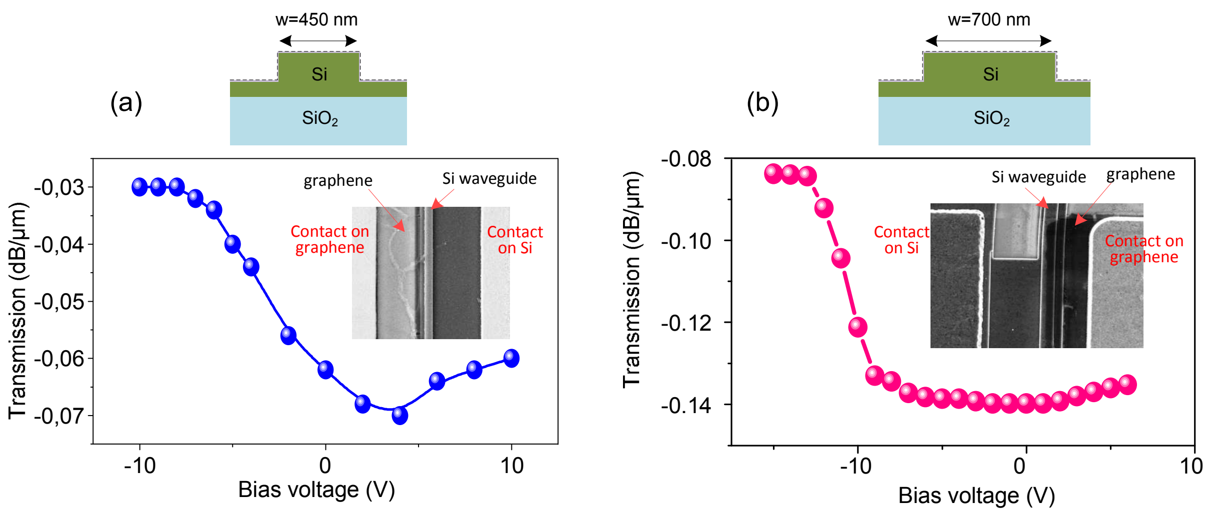

Fig. S6. Experimental analysis on the tunability of graphene-silicon straight waveguide as a finction of bias voltage for the (a) TE and (b) TM mode. The inset shows the fabricated device.

A silicon microring with 700 nm wide waveguide is fabricated. The transmission of the TM mode is measured, as shown in Fig. S7. Very complicated transmission is however obtained, indicating higher mode resonances.

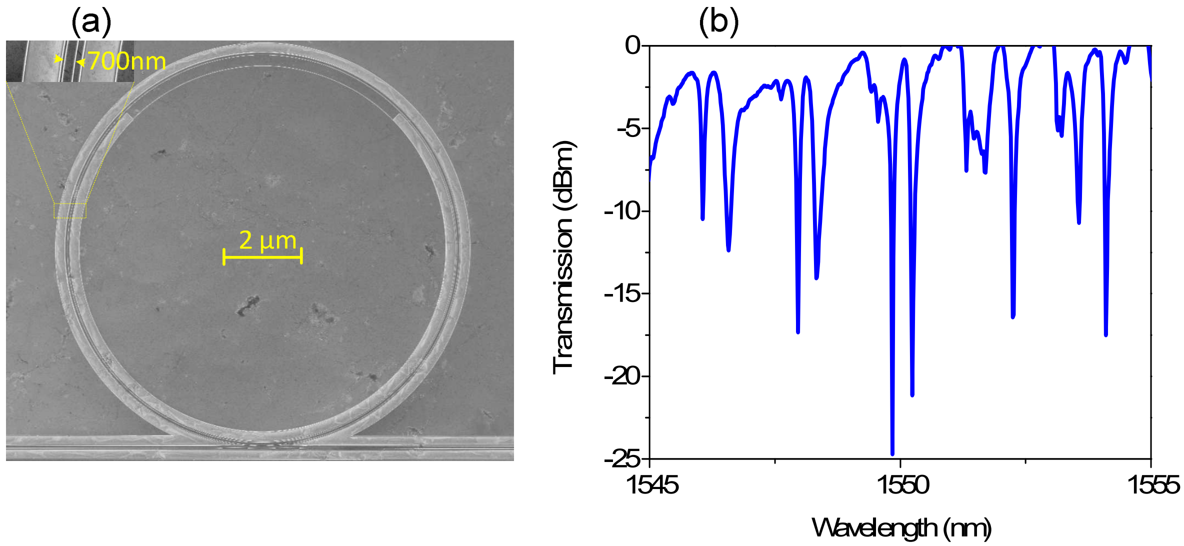

Fig. S7. (a) Fabricated microring resonator with 700nm wide waveguide. The inset shows the dimension of the bend waveguide. (b) Measured transmission of the TM mode for a silicon microring with waveguide width of 700 nm.

7. References

S1. Gao, W. L.; Shu, J.; Qiu, C. Y.; Xu, Q. F. Excitation of plasmonic waves in graphene by guided-mode resonances. *ACS Nano* **2012**, 6, 7806−7813.

S2. Kim, J.; Son, H.; Cho, D. J.; Geng, B. S.; Regan, W.; Shi, S. F.; Kim, K.; Zettl, A.; Shen, Y. R.; Wang, F., Electrical Control of Optical Plasmon Resonance with Graphene, *Nano Lett.* **2012**, 12, 5598−5602.

S3. Bogaerts, W.; De Heyn, P.; Van Vaerenbergh, T.; De Vos, K.; Kumar Selvaraja, S.; Claes, T.; Dumon, P.; Bienstman, P.; Van Thourhout, D.; Baets, R. Silicon microring resonators. *Las. Photon. Rev.* **2012**, 6, 47−73.

S4. Hu, Y.T.; Pantouvaki, M.; Brems, S.; Asselberghs, I.; Huyghebaert, C.; Geisler, M.; Alessandri, C.; Baets, R.; Absil, P.; Van Thourhout, D.; Van Campenhout, J. Broadband 10Gb/s Graphene

Electro-Absorption Modulator on Silicon for Chip-Level Optical Interconnects, *IEEE International Electron Devices Meeting (IEDM)*, San Francisco, CA, Dec. **2014**, 5.6.1−5.6.4.